A Hybrid Approach for the Simulation of the Thermal Motion of a Nearly Neutrally Buoyant Nanoparticle in an Incompressible Newtonian Fluid Medium

B. Uma
Department of Anesthesiology and Critical Care,
University of Pennsylvania,
Philadelphia, PA 19104
e-mail: umab@seas.upenn.edu

R. Radhakrishnan
Department of Bioengineering,
University of Pennsylvania,
Philadelphia, PA 19104
e-mail: rradhak@seas.upenn.edu

D. M. Eckmann
Department of Anesthesiology and Critical Care,
University of Pennsylvania,
Philadelphia, PA 19104
e-mail: David.Eckmann@uphs.upenn.edu

P. S. Ayyaswamy[1]
Department of Mechanical Engineering
and Applied Mechanics,
University of Pennsylvania,
Philadelphia, PA 19104
e-mail: ayya@seas.upenn.edu

A hybrid approach consisting of a Markovian fluctuating hydrodynamics of the fluid and a non-Markovian Langevin dynamics with the Ornstein–Uhlenbeck noise perturbing the translational and rotational equations of motion of a nanoparticle is employed to study the thermal motion of a nearly neutrally buoyant nanoparticle in an incompressible Newtonian fluid medium. A direct numerical simulation adopting an arbitrary Lagrangian–Eulerian based finite element method is employed for the simulation of the hybrid approach. The instantaneous flow around the particle and the particle motion are fully resolved. The numerical results show that (a) the calculated temperature of the nearly neutrally buoyant Brownian particle in a quiescent fluid satisfies the equipartition theorem; (b) the translational and rotational decay of the velocity autocorrelation functions result in algebraic tails, over long time; (c) the translational and rotational mean square displacements of the particle obey Stokes–Einstein and Stokes–Einstein–Debye relations, respectively; and (d) the parallel and perpendicular diffusivities of the particle closer to the wall are consistent with the analytical results, where available. The study has important implications for designing nanocarriers for targeted drug delivery. A major advantage of our novel hybrid approach employed in this paper as compared to either the fluctuating hydrodynamics approach or the generalized Langevin approach by itself is that only the hybrid method has been shown to simultaneously preserve both hydrodynamic correlations and equilibrium statistics in the incompressible limit.
[DOI: 10.1115/1.4007668]

Keywords: nanocarrier motion, fluctuating hydrodynamics, generalized Langevin dynamics, hybrid numerical simulation, targeted drug delivery

1 Introduction

The chief motivation for the present study is the simulation of the thermal motion of a nanoparticle in a fluid flow that occurs in targeted drug delivery [1–6] where the drug carrying nanocarriers are intravascularly introduced into the vasculature. Nanoparticles allow more precise and successful infiltration of drugs to target cells. In general, nanoparticle drug-delivery systems have been shown to enhance the solubility of compounds, and to reduce the impact of drugs on nontarget tissue, thereby eliminating unwanted and dangerous side effects. In order to more broadly integrate this technology into medicine, a precise understanding of how to guide the nanoparticle to the target site is necessary. To achieve this goal, as a first step, it is necessary to determine the motion of a nanocarrier (due to thermal and hydrodynamic effects) in a fluid medium. The nanocarrier with a loaded cargo may be studied subsequently.

A nanoparticle suspended in a fluid undergoes random motion due to the thermal fluctuations in the fluid. As a consequence, translational and rotational degrees of freedom become important. In determining the translational and rotational motions of the nanoparticle in an incompressible Newtonian medium, there exist two methods that couple the thermal fluctuations with the hydrodynamic interactions. These are the generalized Langevin method [7] and the fluctuating hydrodynamics method [8]. Either procedure would require numerical simulations for covering extensive parameter space.

In the fluctuating hydrodynamics approach, the nanoparticle motion incorporates both the Brownian motion and the effect of hydrodynamic force acting on its surface imparted from the surrounding fluid. This method essentially consists of adding stochastic stresses (random stress) to the stress tensor in the momentum equation of the fluid and stochastic fluxes to the heat flux where the energy equation is present [9]. The stochastic stress tensor depends on the temperature and the transport coefficients of the fluid medium [10,11]. Numerical simulations of the fluctuating hydrodynamics approach have been carried out employing the finite volume method [12–14], Lattice-Boltzmann method [15–21], finite element method [8,22,23] and stochastic immersed boundary method [24].

In the Langevin dynamics method, the effect of thermal fluctuations are incorporated as random forces and torques in the particle equation of motion [7,25–30]. The properties of these forces depend on the grand resistance tensor. The tensor in turn depends on the fluid properties, particle shape, and its instantaneous location such as its proximity to a wall or a boundary. This is a robust thermostat, which preserves equilibrium distributions at constant temperatures (i.e., adheres to the equipartition theorem). Clearly,

[1]Corresponding author.

Manuscript received March 28, 2012; final manuscript received May 21, 2012; published online December 6, 2012. Assoc. Editor: Gerard F. Jones.

coupling to a thermostat will alter the hydrodyamics of the nanoparticle system. The characterizations of the performance of the thermostat as well as how it alters the associated hydrodynamic correlations are important. Numerical schemes for studying the nanoparticle motion in a fluid must simultaneously consider the momentum (Langevin) equation for the particle and the Navier–Stokes equation for the fluid. The random force/torque in the particle equation can then be related to the frictional force/torque via the generalized fluctuation–dissipation theorem [31,32]. The implementation can occur in two ways: (i) directly adjust the variance of the random force term in the classical Langevin equation to play the role of a thermostat and (ii) a second, more direct approach that preserves the structure of the generalized Langevin equation, is to consider the power spectrum for the variance of the random force term using a correlated or colored noise with a well defined characteristic memory time. Such a formalism simultaneously preserves the equipartition theorem and the nature of the long time hydrodynamic correlations, and proves to be a versatile thermostat [7].

The fluctuating hydrodynamics approach in an incompressible fluid [8] captures the correct hydrodynamic correlations and conserves thermal equipartition only after adding the mass correction [10]. On the other hand, the generalized Langevin dynamics yields the correct thermal equipartition (without any mass correction), but modifies the nature of the hydrodynamics correlations (due to the coupling of the fluid equations with the thermostat degrees of freedom) [7].

Recently, we have formulated a novel hybrid approach combining Markovian fluctuating hydrodynamics of the fluid and the non-Markovian Langevin dynamics with the Ornstein–Uhlenbeck noise perturbing the translational and rotational equations of motion of the nanocarrier [33]. For this hybrid approach, we have verified the conservation of thermal equipartition and the nature of hydrodynamic correlations by comparisons with well-known analytical results [10]. This approach effectively produces a thermostat that also simultaneously preserves the true hydrodynamic correlations [33]. With this procedure, we have also evaluated adhesive interactions between a receptor on the nanocarrier surface and a ligand (tethered by a spring force) on the surface of an endothelial cell lining the cylindrical vessel wall at a specified finite temperature [34].

In this paper, we demonstrate the thermal equilibrium and hydrodynamic correlations of a nearly neutrally buoyant nanoparticle using our recently developed hybrid approach. A direct numerical simulation procedure adopting an arbitrary Lagrangian–Eulerian based finite element method is employed to simulate the Brownian motion of a nearly neutrally buoyant particle in an incompressible Newtonian fluid contained in a horizontal micron sized cylindrical vessel. The results for the attainment of thermal equilibrium between the particle and the surrounding medium, diffusivity for the particle in the medium, effect of the presence of the confining vessel wall on particle displacement and diffusivity are evaluated and discussed in detail.

A major advantage of our novel hybrid approach employed in this paper as compared to either the fluctuating hydrodynamics approach or the generalized Langevin approach by itself is that only the hybrid method has been shown to simultaneously preserve both hydrodynamic correlations and equilibrium statistics in the incompressible limit.

2 Formulation of the Problem

The Brownian motion of a nearly neutrally buoyant nanoparticle in an incompressible Newtonian stationary fluid medium contained in a horizontal circular vessel is considered. The fluid and particle equations are formulated in an inertial frame of reference with the origin coinciding with the center of the vessel (Fig. 1). The radius, R, and the length, L, of the vessel (tube) are very large compared to the particle size, a, the radius of the particle. Initially, the nanoparticle is introduced either at the vessel centerline or at suitably chosen locations away from the center line toward the bounding wall. Initially both the fluid and particle are at rest. No body force is considered either for the particle or for the fluid domain. At time $t=0$, the nanoparticle is subjected to Brownian motion. The motion of the nanoparticle is determined by the hydrodynamic forces and torques acting on the particle and the wall interactions.

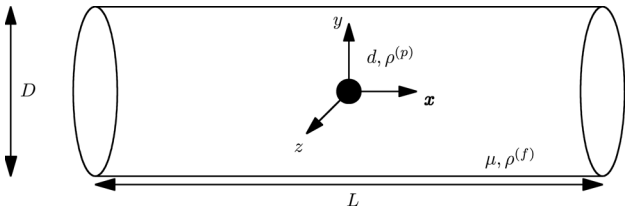

Fig. 1 Schematic representation of a nanoparticle in a cylindrical vessel (tube) (not to scale). Radius of the tube: $R=5\,\mu$m; length of the tube: $L=10\,\mu$m; radius of the nanoparticle: $a=250$ nm; viscosity of the fluid: $\mu=10^{-3}$ kg/ms; density of the fluid and the nanoparticle: $\rho^{(f)}=10^3$ kg/m^3, 990 kg/m$^3 \le \rho^{(p)} \le 1010$ kg/m^3.

2.1 Hybrid Scheme: Governing Equations and Boundary Conditions. The motion of an incompressible Newtonian fluid satisfies the conservation of mass and momentum given by

$$\nabla \cdot \boldsymbol{u} = 0; \quad \rho^{(\mathrm{f})}(\boldsymbol{u}_t + (\boldsymbol{u}\cdot\nabla)\boldsymbol{u}) = \nabla\cdot\boldsymbol{\sigma} \tag{1}$$

$$\boldsymbol{\sigma} = -p\boldsymbol{J} + \mu\left[\nabla\boldsymbol{u} + (\nabla\boldsymbol{u})^T\right] + \boldsymbol{S} \tag{2}$$

where $\boldsymbol{u}$ and $\rho^{(\mathrm{f})}$ are the velocity and density of the fluid, respectively, $\boldsymbol{\sigma}$ is the stress tensor, p is the pressure, $\boldsymbol{J}$ is the identity tensor, and μ is the dynamic viscosity. The random stress tensor $\boldsymbol{S}$ is assumed to be a Gaussian with

$$\begin{aligned} \langle S_{ij}(\boldsymbol{x},t)\rangle &= 0 \quad \text{and} \\ \langle S_{ik}(\boldsymbol{x},t)S_{lm}(\boldsymbol{x}',t')\rangle &= 2k_{\mathrm{B}}T\mu(\delta_{il}\delta_{km}+\delta_{im}\delta_{kl}) \\ &\quad \delta(\boldsymbol{x}-\boldsymbol{x}')\delta(t-t') \end{aligned} \tag{3}$$

where $\langle\ \rangle$ is the ensemble average, k_{B} is the Boltzmann constant, T is the absolute temperature, δ_{ij} is the Kronecker delta, and the Dirac delta function $\delta(\boldsymbol{x}-\boldsymbol{x}')$ denotes that the components of the random stress tensor are spatially uncorrelated (Markovian). The right hand side of Eq. (3) denotes the mean and variance of the thermal fluctuations chosen to be consistent with the fluctuation–dissipation theorem [9,10,35,36]. By including this stochastic stress tensor due to the thermal fluctuations in the governing equations, the macroscopic hydrodynamic theory is generalized to include the mesoscopic scales ranging from tens of nanometers to a few microns.

For a rigid particle suspended in an incompressible Newtonian fluid, the translational and rotational motions of the particle satisfies Newton's second law and the Euler equation, respectively. In the hybrid formulation, the time correlated noise is added into the particle equations of motion [33,34]

$$m\frac{d\boldsymbol{U}}{dt} = -\int_{\partial\Sigma_{\mathrm{p}}} \boldsymbol{\sigma}\cdot\hat{\boldsymbol{n}}\,ds + \int_{-\infty}^{t_-} \xi(t')e^{-|t-t'|/\tau_1}dt' \tag{4}$$

$$\frac{d(\boldsymbol{I}\boldsymbol{\omega})}{dt} = -\int_{\partial\Sigma_{\mathrm{p}}} (\boldsymbol{x}-\boldsymbol{X})\times[\boldsymbol{\sigma}\cdot\hat{\boldsymbol{n}}]ds + \int_{-\infty}^{t_-} \boldsymbol{\eta}(t')e^{-|t-t'|/\tau_2}dt' \tag{5}$$

where m is the mass of the particle, $\boldsymbol{I}$ is its moment of inertia, $\boldsymbol{U}$ and $\boldsymbol{\omega}$ are the translational and angular velocities of the particle, respectively, $\boldsymbol{X}$ is the position of the centroid of the particle, $(\boldsymbol{x}-\boldsymbol{X})$ is a vector from the center of the particle to a point on its

surface, $\partial\Sigma_p$ denotes the particle surface, $\hat{\boldsymbol{n}}$ is the unit normal vector on the surface of the particle pointing into the particle, and the random force $\boldsymbol{\xi}$ and torque $\boldsymbol{\eta}$ are given by

$$\boldsymbol{\xi}(t') = \int_{\partial\Sigma_p} \boldsymbol{S}(\boldsymbol{x}', t') \cdot \hat{\boldsymbol{n}}\, ds \tag{6}$$

$$\boldsymbol{\eta}(t') = \int_{\partial\Sigma_p} (\boldsymbol{x}' - \boldsymbol{X}) \times (\boldsymbol{S}(\boldsymbol{x}', t') \cdot \hat{\boldsymbol{n}}) ds \tag{7}$$

for the Ornstein–Uhlenbeck process. The time integral in Eqs. (4) and (5) excludes the frictional force and torque at the time instant t since it has already been accounted for in the hydrodynamic force and torque terms, respectively. The characteristic memory time for translational, $\tau_1 = n_1 \cdot \Delta t$, and rotational, $\tau_2 = n_2 \cdot \Delta t$, motions of the nanoparticle add certain amounts of memory from the previous history of fluctuations to the system. Here, Δt is the time step for the numerical simulation, n_1 and n_2 correspond to the number of time steps required to adequately represent the memory effects. These are variable quantities and are determined on the basis of satisfying the equipartition theorem. The amount of memory required by translational and rotational motions of the nanoparticle in order to satisfy the equipartition theorem are different. Hence, $\tau_1 = \tau_2$ is not a necessary condition for the temperature of the particle to attain the preset temperature of the fluid. Equations (6) and (7) are the random force and torque acting on the nanoparticle at time t' (a previous time instant). Since the random stress $\boldsymbol{S}(\boldsymbol{x}, t)$ is Gaussian, $\boldsymbol{\xi}(t')$ and $\boldsymbol{\eta}(t')$ are also Gaussian with variance equivalent to the strength of the white noise in the Langevin equation. In the limit of the characteristic memory times $\tau_1, \tau_2 \to 0$ (i.e., in the absence of memory), Eqs. (4) and (5) reduce to the Newton's second law and the Euler equations, respectively, which correspond to the Markovian fluctuating hydrodynamics.

The initial and boundary conditions for the problem are

$$\boldsymbol{U}(t=0) = 0; \quad \boldsymbol{u}(t=0) = 0 \quad \text{on} \quad \Sigma_0 - \partial\Sigma_i \tag{8}$$

$$\boldsymbol{u} = 0 \quad \text{on} \quad \partial\Sigma_i; \quad \boldsymbol{\sigma} \cdot \hat{\boldsymbol{n}} = 0 \quad \text{on} \quad \partial\Sigma_o \tag{9}$$

$$\boldsymbol{u} = \boldsymbol{U} + \boldsymbol{\omega} \times (\boldsymbol{x} - \boldsymbol{X}) \quad \text{on} \quad \partial\Sigma_p \tag{10}$$

where Σ_0 is the domain occupied by the fluid and $\partial\Sigma_i$ and $\partial\Sigma_o$ are the inlet and outlet boundaries, respectively. The stochastic governing Eqs. (1)–(5) along with the initial and boundary conditions (8)–(10) are solved numerically. It is assumed that there is no body torque acting at any point in the fluid and the viscous stress tensor, σ, is symmetric.

A numerical simulation at a mesoscopic scale involving a particle in a fluid could be based on a discretization of the Eqs. (1)–(10). However, the discrete forms have to satisfy the fluctuation–dissipation theorem [11–13,35–38]. Español and Zúñiga [22] and Español et al. [23] have shown that a well behaved set of discrete equations obtained in terms of the finite element shape functions based on the Delaunay triangulation conserves mass, momentum and energy while ensuring thermodynamic consistency. In the present study, we obtain the discrete hydrodynamic equations using finite element shape functions based on the Delaunay–Voronoi tetrahedrizations. The computational domain is covered by a finite element mesh generated using Delaunay–Voronoi methods. The fluid domain is discretized by quadratic irregular tetrahedral elements. A typical element is shown in Fig. 2. Figure 3 shows a triangular mesh discretizing the surface of the fluid domain (cylinder) and the surface of the nanoparticle. The discretization of the fluid domain changes at each time step of the simulation due to the motion of the nanoparticle. The procedure for numerical simulation of the random stresses associated with the unstructured tetrahedron mesh while conserving the volume is described in detail in Uma et al. [8]. The details of combined fluid–solid weak formulation, spatial discretization,

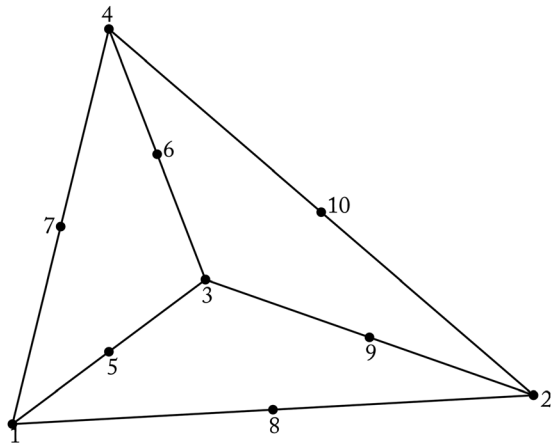

Fig. 2 Representation of a ten-node tetrahedron

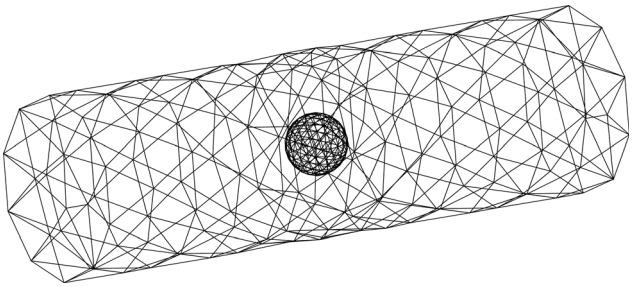

Fig. 3 Finite element surface mesh of a cylindrical tube with one spherical nanoparticle

mesh movement techniques, and temporal discretization of time derivatives are discussed in Refs. [7] and [8]. These details will not be repeated here for brevity. Briefly, the fluid domain is approximated by quadratic tetrahedral finite-elements (ten nodes defined per tetrahedron with ten basis functions that are second-order polynomials). The discrete solution for the fluid velocity is approximated in terms of piecewise quadratic functions, and is assumed to be continuous over the domain (P2 elements). The discrete solution for the pressure is taken to be piecewise linear and continuous (P1 element). This P1/P2 element for the pressure and velocity is consistent with the Ladyzhenskaya–Babuska–Brezzi (LBB) or inf–sup condition and yields convergent solutions [39,40].

The time scales involved in this study are (i) $\tau_b = m/\zeta^{(t)}$, the Brownian relaxation time over which velocity correlations decay in the Langevin equation, (ii) $\tau_d = a^2\zeta^{(t)}/k_BT$, the Brownian diffusive time scale over which the nanoparticle diffuses over a distance equal to its own radius, and (iii) $\tau_\nu = a^2/\nu$, the hydrodynamic time scale for momentum to diffuse over a distance equal to the radius of the nanoparticle, where $\zeta^{(t)} = 6\pi\mu a$ is the Stokes dissipative friction force coefficient for a sphere; a is the radius of the nanoparticle, and ν is the kinematic viscosity of the fluid. The time step Δt for the numerical simulation has been chosen to be smaller than all the relevant physical time scales described above. The simulations presented in this study have been carried out for long enough durations to allow for the temperature of the particle to equilibrate; i.e., if N is the number of simulated time steps then $N \cdot \Delta t = t \gg \tau_\nu$.

3 Numerical Results and Discussion

A nearly neutrally buoyant solid spherical particle of radius $a = 250$ nm is placed at the center of a cylindrical tube ($R = 5\ \mu$m) containing a quiescent Newtonian fluid. The temperature of the fluid is initially set to $T = 310$ K. For a given nanoparticle of radius a, and tube radius R, a "realization" consists of N time steps

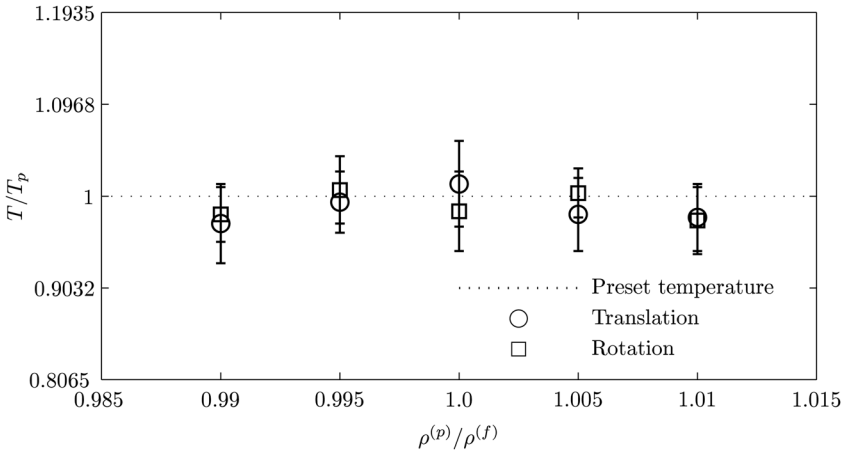

Fig. 4 Translational and rotational temperatures of a nearly neutrally buoyant nanoparticle in a stationary fluid medium as a function of the particle density normalized with fluid density. The nondimensionalized characteristic memory times are $\tau_1/\tau_v = 0.12$ and $\tau_2/\tau_v = 0.088$.

(approximately 10 s wall clock time for each time step that is generally considered in this study). The number of time steps depends upon equilibration of particle temperature, or determination of velocity autocorrelations (VACFs) and mean square displament (MSD). In order to ensure the uniqueness of the realizations, different initial seeds are chosen for a Gaussian random number generator. In this section, we numerically predict (i) the translational and rotational temperatures of the nanoparticle, where the temperature calculation is carried out until thermal equilibration is obtained for the particle; (ii) the translational and rotational velocity distributions of the nanoparticle motion; (iii) the translational and rotational VACFs; (iv) the translational and rotational MSD of the particle for both ballistic and diffusive regimes; and (v) the effects of the presence of the bounding wall on particles of different radii initially placed at various locations are evaluated for several cases without bulk flow. We compare the various numerical predictions with known analytical results, where available.

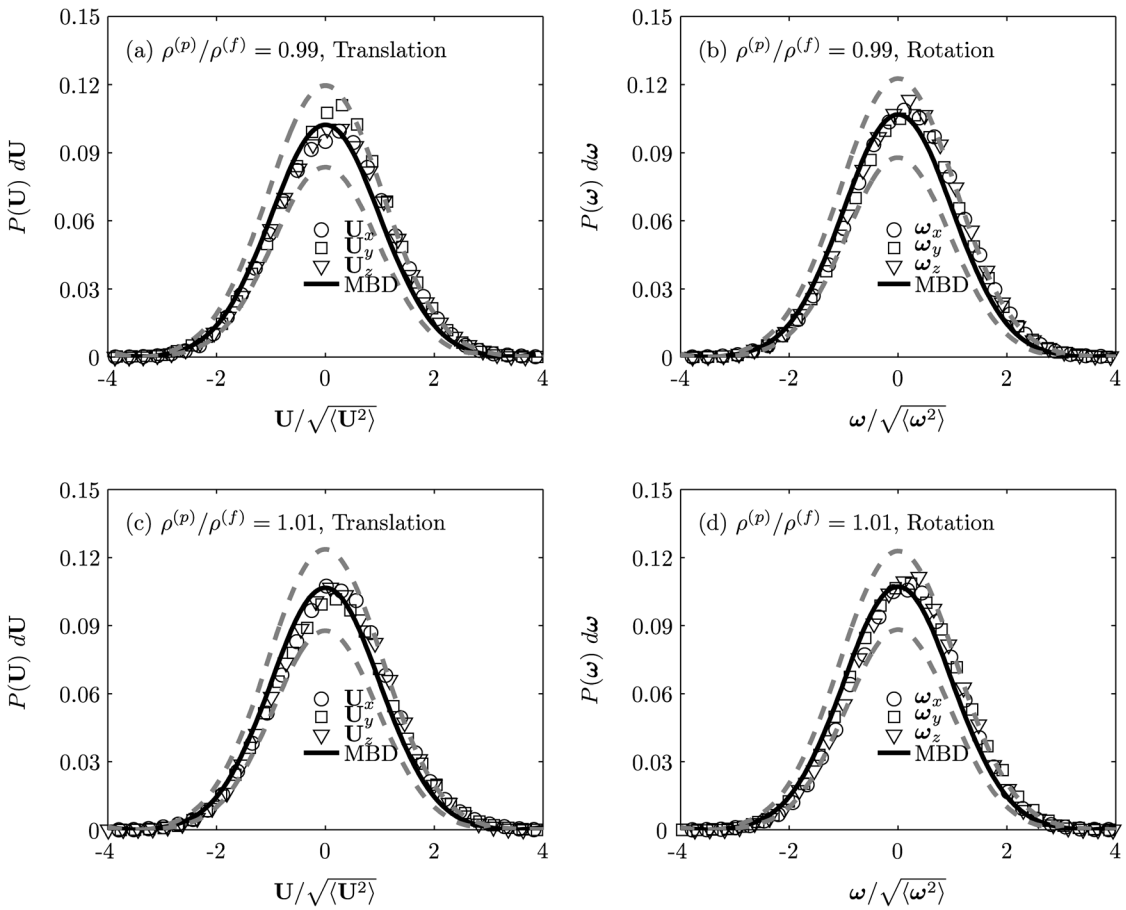

Fig. 5 Equilibrium probability of the (*a*) and (*c*) translational and (*b*) and (*d*) rotational velocities of the nanoparticle in a stationary Newtonian fluid medium for $\rho^{(p)}/\rho^{(f)} = 0.99$ ((*a*) and (*b*)) and 1.01 ((*c*) and (*d*)). The nondimensionalized characteristic memory times are $\tau_1/\tau_v = 0.12$ and $\tau_2/\tau_v = 0.088$ [33].

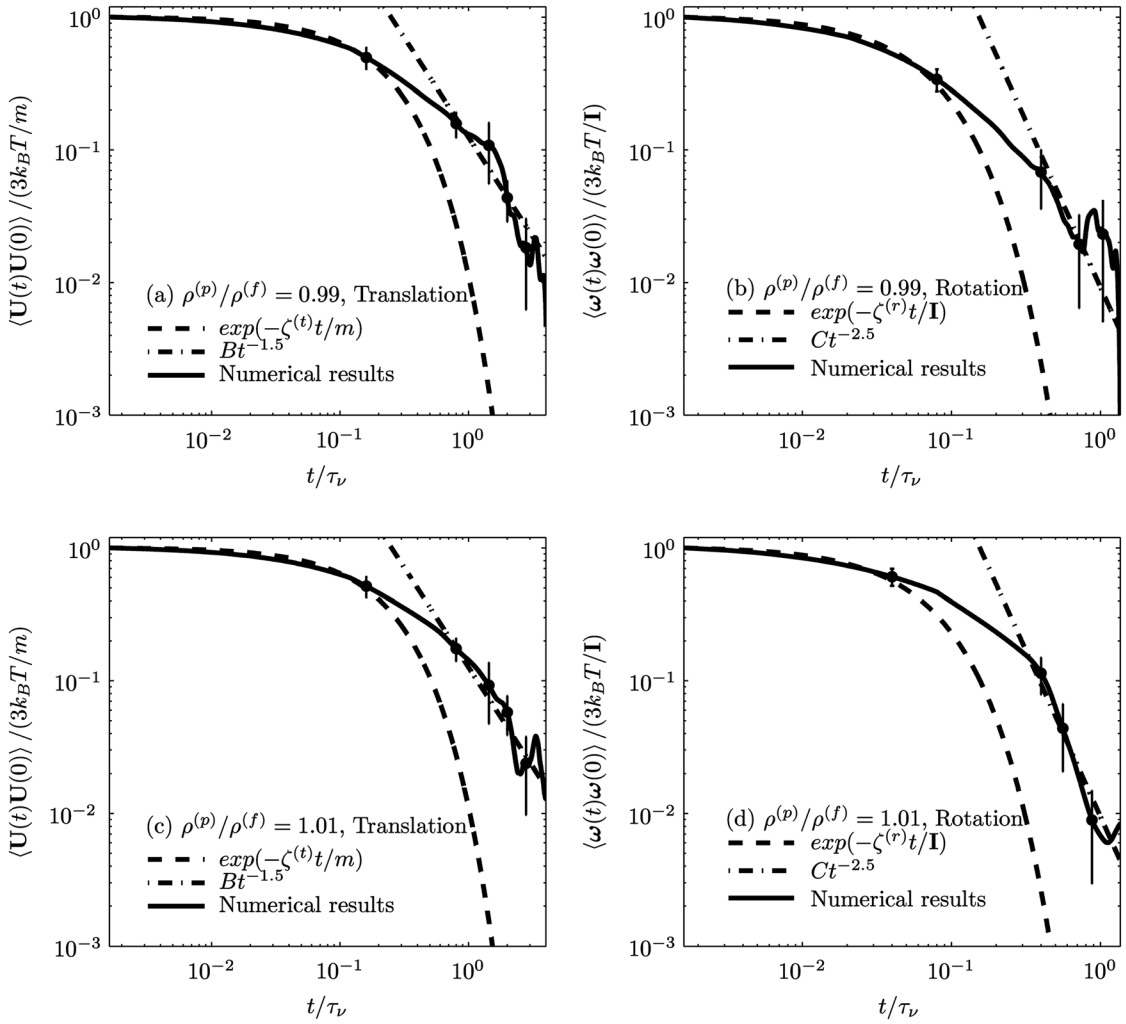

Fig. 6 (*a*) and (*c*) Translational ($B = m\rho^{(f)1/2}/12\pi^{3/2}\mu^{3/2}$) and (*b*) and (*d*) rotational ($C = I\rho^{(f)3/2}/32\pi^{3/2}\mu^{5/2}$) VACFs of the Brownian particle ($a = 250$ nm) in a fluid medium through a circular vessel using hybrid approach. The nondimensionalized characteristic memory times are $\tau_1/\tau_\nu = 0.12$ and $\tau_2/\tau_\nu = 0.088$ [33].

3.1 Equipartition Theorem. Figure 4 shows that translational and rotational temperatures of nearly neutrally buoyant Brownian particles, thermally equilibrated, in a quiescent fluid medium are independent of the density of the particle in relation to that of fluid. The nondimensionalized characteristic memory times $\tau_1/\tau_\nu = 0.12$ and $\tau_2/\tau_\nu = 0.088$ [33]. The error bars have been plotted from standard deviations of the temperatures obtained with 15 different realizations.

3.2 Maxwell–Boltzmann Distribution. Figure 5 shows the numerically simulated components of $\boldsymbol{U}$ (Figs. 5(*a*) and 5(*c*)) and $\boldsymbol{\omega}$ (Figs. 5(*b*) and 5(*d*)) (represented by three different symbols) of the nearly neutrally buoyant nanoparticle ($a = 250$ nm) are compared with the analytical form of the Maxwell–Boltzmann distribution (MBD) with a zero mean and variance of k_BT/m and $k_BT/\boldsymbol{I}$, respectively. The nondimensionalized characteristic memory times are $\tau_1/\tau_\nu = 0.12$ and $\tau_2/\tau_\nu = 0.088$ [33]. It is observed that each degree of freedom individually follows MBD within 5% error (see dotted line in Fig. 5). This validates the numerical procedure employed in this study.

3.3 Hydrodynamic Correlations. A nanoparticle experiencing Brownian motion in a fluid is influenced by the hydrodynamic interactions. The fluid around the particle is dragged in the direction of motion of the particle. On the other hand, the motion of the particle is resisted by viscous forces arising due to its motion relative to the surrounding fluid. The momentum of the fluid surrounding the particle at any instant is related to its recent history. The friction coefficient is time dependent and is no longer given by the constant (steady flow) Stokes value.

Hauge and Martin-Löf [10] have analytically shown that the decay of the translational and rotational VACFs at long time obeys a power-law:

$$\frac{\langle \boldsymbol{U}(t)\boldsymbol{U}(0)\rangle}{\langle \boldsymbol{U}(0)\boldsymbol{U}(0)\rangle} \simeq \left(\frac{m\rho^{(f)1/2}}{12\pi^{3/2}\mu^{3/2}}\right)t^{-3/2} = Bt^{-3/2} \tag{11}$$

$$\frac{\langle \boldsymbol{\omega}t)\boldsymbol{\omega}(0)\rangle}{\langle \boldsymbol{\omega}(0)\boldsymbol{\omega}(0)\rangle} \simeq \left(\frac{\boldsymbol{I}\rho^{(f)3/2}}{32\pi^{3/2}\mu^{5/2}}\right)t^{-5/2} = Ct^{-5/2} \tag{12}$$

As for the short time behavior, the VACF is expected to adhere to the Langevin (white noise) limit [41]: for translation VACF $\sim \exp(-\zeta^{(t)}t/m)$, and for rotation VACF $\sim \exp(-\zeta^{(r)}t/I)$, where $\zeta^{(r)} = 8\pi\mu a^3$.

Figure 6 shows the VACF of the translational and rotational motions of the nearly neutrally buoyant nanoparticle ($a = 250$ nm) in a quiescent fluid medium in a circular vessel as obtained from our numerical simulations. For determining the VACF of the nanoparticle, 15 different realizations have been employed with total computation of $15 \times 100,000 = 1,500,000$ time steps. For this calculation, characteristic memory times are $\tau_1/\tau_\nu = 0.12$ and $\tau_2/\tau_\nu = 0.088$ [33]. For the parameters considered in this

study, our numerical simulations predict that the translational and rotational VACFs follow an exponential decay at short times and an algebraic tail at long times. Furthermore, the algebraic decay of the translational and rotational VACFs have power-law behavior characterized by $\sim t^{-3/2}$ and $\sim t^{-5/2}$, respectively. The error bars have been plotted from standard deviations of the decay at particular time instants obtained with 15 different realizations. Hence, our computed numerical results for nearly neutrally buoyant nanoparticle based on the hybrid non-Markovian fluctuating hydrodynamics approach are in good agreement with the predictions for short and long times (Eqs. (11) and (12)), respectively.

3.4 Diffusion of the Nanoparticle. For the Langevin equation of a Brownian particle

$$m\frac{d\mathbf{U}}{dt} = -\zeta^{(\mathrm{t})}\mathbf{U} + \mathbf{R}(t) \tag{13}$$

the translational and rotational MSDs of the nanoparticle at long times satisfy the Stokes–Einstein [42,43] and the Stokes–Einstein–Debye relations [44], respectively, given by

$$\left\langle |\mathbf{X}(\Delta t) - \mathbf{X}_0|^2 \right\rangle = 6D_\infty^{(\mathrm{t})}\Delta t; \quad D_\infty^{(\mathrm{t})} = \frac{k_\mathrm{B}T}{\zeta^{(\mathrm{t})}} \tag{14}$$

$$\left\langle |\boldsymbol{\theta}(\Delta t) - \boldsymbol{\theta}_0|^2 \right\rangle = 6D_\infty^{(\mathrm{r})}\Delta t; \quad D_\infty^{(\mathrm{r})} = \frac{k_\mathrm{B}T}{\zeta^{(r)}}; \quad \zeta^{(\mathrm{r})} = 8\pi\mu a^3 \tag{15}$$

Here $\mathbf{X}_0$ is the initial location of the particle, $\mathbf{X}(\Delta t)$ is its linear displacement at time Δt, $\boldsymbol{\theta}(\Delta t)$ is its angular displacement at time Δt, and $D_\infty^{(\mathrm{t})}$ and $D_\infty^{(\mathrm{r})}$ are the translational and rotational self-diffusion coefficients of the Brownian particle at long times, respectively.

Figure 7 shows the numerically obtained translational and rotational MSDs (measures of diffusion) of a nearly neutrally buoyant nanoparticle ($a = 250\,\mathrm{nm}$) in a quiescent fluid medium, initially placed at the center of the vessel ($R = 5\,\mu\mathrm{m}$), for both short and long times. It is observed that in the regime where the particle's motion is dominated by its own inertia (ballistic), the translational and rotational motions of the particle follow $(3k_\mathrm{B}T/m)t^2$ and $(3k_\mathrm{B}T/\boldsymbol{I})t^2$, respectively. In the diffusive regime, $t \gg \tau_\mathrm{b}$, the translational and rotational MSDs increase linearly in time to follow $6D_\infty^{(\mathrm{t})}t$ (Stokes–Einstein relation) and $6D_\infty^{(\mathrm{r})}t$ (Stokes–Einstein–Debye relation), respectively, where $D_\infty^{(\mathrm{t})} = k_BT/\zeta^{(\mathrm{t})}$, and $D_\infty^{(\mathrm{r})} = k_BT/\zeta^{(\mathrm{r})}$ ($\zeta^{(\mathrm{r})} = 8\pi\mu a^3$) are the translational and rotational self-diffusion coefficients. The results are obtained from 15 realizations, each realization computed up to 100,000 time steps. The nondimensionalized characteristic memory times are $\tau_1/\tau_\nu = 0.12$ and $\tau_2/\tau_\nu = 0.088$ [33].

3.5 Wall Effects. As stated earlier, our main motivation for the present study is to simulate a nearly neutrally buoyant nanoparticle thermal motion in a fluid flow that occurs in targeted drug delivery and similar microparticle flows. In such flows, the hydrodynamic wall effects on the particle diffusivity are relevant. For a particle initially located at the center of the cylindrical vessel, the wall effects play a minimal role ($\leq 3\%$, compared to an unbounded fluid domain) on the diffusion coefficient (see Fig. 7) [45]. When a particle of radius a is initially placed at a distance h from the tube wall to the center of the particle, $h < R$, the

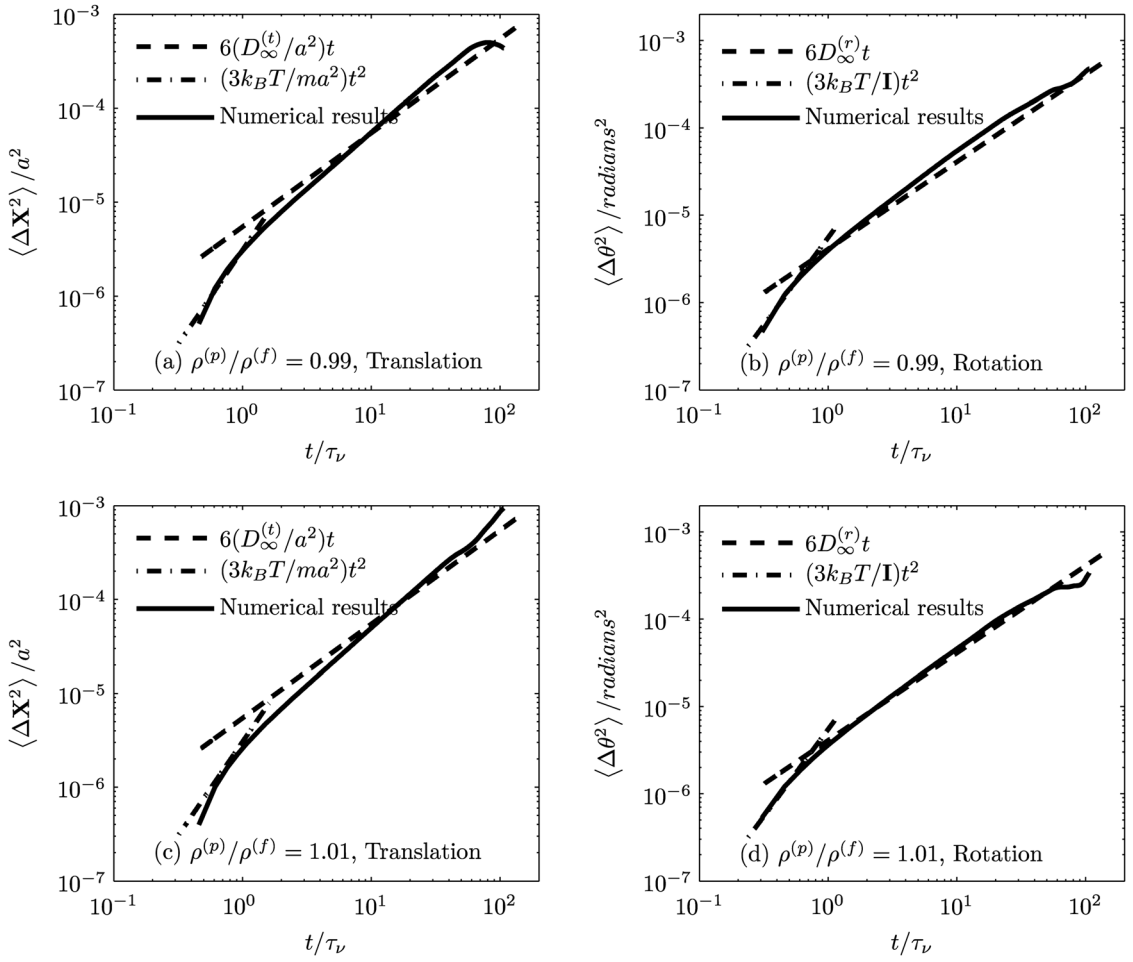

Fig. 7 The MSD of a nearly neutrally buoyant Brownian particle ($a = 250\,\mathrm{nm}$) in a stationary fluid medium using hybrid approach. The nondimensionalized characteristic memory times are $\tau_1/\tau_\nu = 0.12$ and $\tau_2/\tau_\nu = 0.088$ [33].

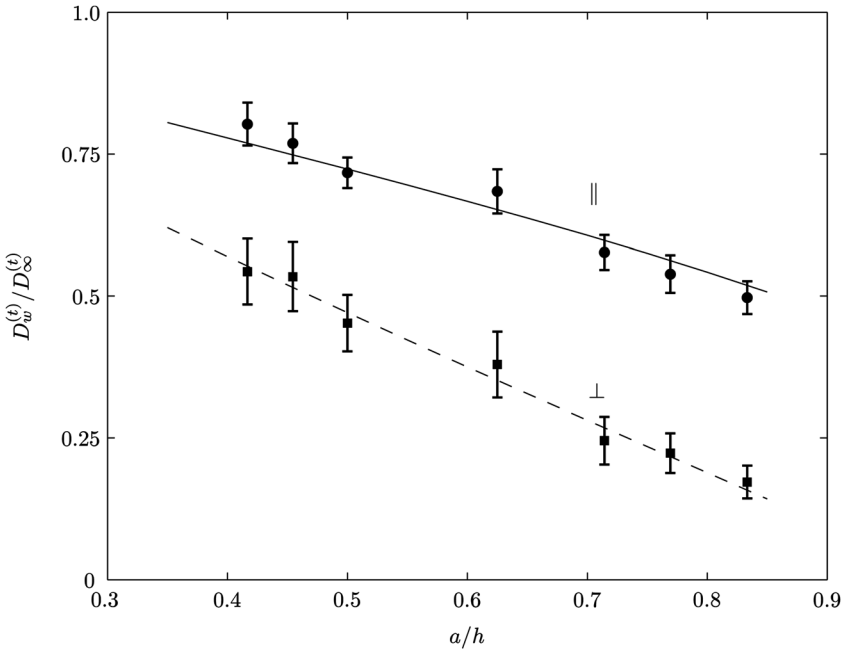

Fig. 8 The translational diffusion coefficient of nearly neutrally buoyant Brownian particles of different radii *a* initially placed at different locations *h* from the wall of the circular vessel in a quiescent medium. Solid and dashed lines correspond to the perturbation solutions given in Happel and Brenner [45].

particle–wall interactions modify the particle diffusivity. For $a \ll R$, in a quiescent fluid, the Brownian motion near the vessel wall is similar to that of motion in the vicinity of a plane wall (curvature effects may be neglected) [45,46]. For a particle initially located in the near vicinity of the wall, there is reduced space for the surrounding fluid to negotiate the particle, and the corresponding drag force in a direction parallel to the wall is higher. The diffusivity of the particle in the proximity of the wall may be estimated to be $D_{\mathrm{w}}^{(\mathrm{t})} = D_{\infty}^{(\mathrm{t})}(\zeta_{\mathrm{w}}^{(\mathrm{t})}/\zeta^{(\mathrm{t})})^{-1}$ in x, y, and z directions [47], while $\zeta_{\mathrm{w}}^{(\mathrm{t})}$ depends on the particular direction.

Figure 8 shows the numerically obtained parallel (x direction) and perpendicular (y direction) diffusivities of nearly neutrally buoyant particles of different radii initially placed at various distances from the tube wall, in a quiescent medium. As mentioned earlier, in the diffusive regime, the translational MSD of the particle increases linearly with time. We have numerically evaluated the gradient of the linear profile, normalized by the translational self-diffusion coefficient, $D_{\infty}^{(\mathrm{t})}$, plotted as a function of a/h. It is observed that for a given particle of radius a, the diffusivity of the particle decreases closer to the wall (i.e., as $h \to 0$, $D_{\mathrm{w}}/D_{\infty}$ decreases). Similarly, for a given location of the particle from the wall, h, the diffusivity of the particle decreases for the larger particle (i.e., as a increases). The nondimensionalized characteristic memory times are $\tau_1/\tau_\nu = 0.12$ and $\tau_2/\tau_\nu = 0.088$ [33]. Our numerical results are in agreement with the predictions of Happel and Brenner [45].

4 Conclusions

A hybrid approach based on Markovian fluctuating hydrodynamics of the fluid and a non-Markovian Langevin dynamics with the Ornstein–Uhlenbeck noise perturbing the translational and rotational equations of motion of a nearly neturally buoyant nanoparticle is employed to simulate the Brownian motion in an incompressible Newtonian fluid. The translational and rotational motions of the nearly neutrally buoyant nanoparticle in a quiescent fluid medium is considered. At thermal equilibrium, the numerical predictions are validated with analytical results, where available.

We have numerically predicted the following:

(a) The translational and rotational temperatures of a nearly neutrally buoyant particle in a quiscent fluid medium. The temperature calculation is carried out till thermal equilibration is obtained between the particle and the fluid medium.
(b) The translational and rotational velocity distributions of a nearly neutrally buoyant nanoparticle motion in a quiescent fluid medium.
(c) The translational and rotational VACFs of a nearly neutrally buoyant particle in a quiescent fluid. Over long times, the decay of the VACF captures algebraic tails for the translational ($t^{-3/2}$) and the rotational ($t^{-5/2}$) motions of the nanoparticle.
(d) The translational and rotational MSDs of a nearly neutrally buoyant particle in a quiescent fluid, both for ballistic and diffusive regimes. At short times, translational and rotational MSDs in a quiescent fluid are proportional to t^2, and in the diffusive regime ($t \gg \tau_{\mathrm{b}}$), they agree with the Stokes–Einstein and Stokes–Einstein–Debye theories.
(e) The effects of the presence of the bounding wall on a nearly neutrally buoyant particles of different radii initially placed at various locations are evaluated for several cases in a quiscent fluid medium. The translational diffusion coefficients for parallel and perpendicular directions have been displayed. Very good agreement with published results, where available is also displayed.
(f) A major advantage of our novel hybrid approach employed in this paper as compared to either the fluctuating hydrodynamics approach or the generalized Langevin approach by itself is that only the hybrid method has been shown to simultaneously preserve both hydrodynamic correlations and equilibrium statistics in the incompressible limit.

Acknowledgment

This work was sponsored by National Institute of Health (NIH) Grant No. R01 EB006818 (D.M.E.); National Science Foundation

(NSF) Grant No. CBET-0853389. Computational resources were provided in part by the National Partnership for Advanced Computational Infrastructure under Grant No. MCB060006.

Nomenclature

$\boldsymbol{R}$ = radius of the circular vessel
L = length of the circular vessel
a = radius of the nanoparticle
$\boldsymbol{u}$ = velocity of the fluid
$\rho^{(\mathrm{f})}$ = density of the fluid
$\rho^{(\mathrm{p})}$ = density of the nanoparticle
$\boldsymbol{\sigma}$ = stress tensor
p = pressure
$\boldsymbol{J}$ = identity tensor
μ = dynamic viscosity
$\boldsymbol{S}$ = random stress tensor
k_{B} = Boltzmann constant
T = absolute temperature
δ_{ij} = Kronecker delta
δ = Dirac delta
m = mass of the particle
$\boldsymbol{I}$ = moment of inertia of the particle
$\boldsymbol{U}, \boldsymbol{\omega}$ = translational and angular velocities of the particle
$\boldsymbol{X}$ = position of the centroid of the particle
$(\boldsymbol{x} - \boldsymbol{X})$ = vector from the center of the particle to a point on its surface
$\partial\Sigma_{\mathrm{p}}$ = the particle surface
$\partial\Sigma_{\mathrm{i}}$ = inlet boundary
$\partial\Sigma_{\mathrm{o}}$ = outlet boundary
$\hat{\boldsymbol{n}}$ = unit normal vector on the surface of the particle pointing into the particle
ξ = random force
η = random torque
τ_{b} = Brownian relaxation time
τ_{d} = Brownian diffusive time
τ_{ν} = hydrodynamic time
$\zeta^{(\mathrm{t})}, \zeta^{(\mathrm{r})}$ = Stokes dissipative friction force and torque coefficient
τ_1, τ_2 = characteristic memory times

References

[1] Liu, J., Weller, G. E. R., Zern, B., Ayyaswamy, P. S., Eckmann, D. M., Muzykantov, V. R., and Radhakrishnan, R., 2010, "A Computational Model for Nanocarrier Binding to Endothelium Validated Using In Vivo, In Vitro, and Atomic Force Microscopy Experiments," Proc. Ntnl Acad. Sci. U.S.A, **107**, pp. 16530–16535.

[2] Liu, J., Agrawal, N., Calderon, A., Ayyaswamy, P., Eckmann, D., and Radhakrishnan, R., 2011, "Multivalent Binding of Nanocarrier to Endothelial Cells Under Shear Flow," Biophys. J., **101**(2), pp. 319–326.

[3] Liu, J., Bradley, R., Eckmann, D., Ayyaswamy, P., and Radhakrishnan, R., 2011, "Multiscale Modeling of Functionalized Nanocarriers in Targeted Drug Delivery," Curr. Nanosci., **7**(5), pp. 727–735.

[4] Swaminathan, T., Liu, J., Uma, B., Ayyaswamy, P., Radhakrishnan, R., and Eckmann, D., 2011, "Dynamic Factors Controlling Carrier Anchoring on Vascular Cells," IUBMB Life, **63**(8), pp. 640–647.

[5] Liu, J., Agrawal, N., Eckmann, D., Ayyaswamy, P., and Radhakrishnan, R., 2012, "Top-Down Mesoscale Models and Free Energy Calculations of Multivalent Protein-Protein and Protein-Membrane Interactions in Nanocarrier Adhesion and Receptor Trafficking," *Innovations in Biomolecular Modeling and Simulations*, T. Schlick, ed., Royal Society of Chemistry, pp. 272–287.

[6] Muzykantov, V., Radhakrishnan, R., and Eckmann, D., 2012, "Dynamic Factors Controlling Targeting Nanocarriers to Vascular Endothelium," Curr. Drug Metab., **113**, pp. 70–81.

[7] Uma, B., Swaminathan, T. N., Ayyaswamy, P. S., Eckmann, D. M., and Radhakrishnan, R., 2011, "Generalized Langevin Dynamics of a Nanoparticle Using a Finite Element Approach: Thermostating With Correlated Noise," J. Chem. Phys., **135**, p. 114104.

[8] Uma, B., Swaminathan, T. N., Radhakrishnan, R., Eckmann, D. M., and Ayyaswamy, P. S., 2011, "Nanoparticle Brownian Motion and Hydrodynamic Interactions in the Presence of Flow Fields," Phys. Fluids, **23**, p. 073602.

[9] Landau, L. D., and Lifshitz, E. M., 1959, *Fluid Mechanics*, Pergamon Press, London.

[10] Hauge, E. H., and Martin-Löf, A., 1973, "Fluctuating Hydrodynamics and Brownian Motion," J. Stat. Phys., **7**(3), pp. 259–281.

[11] Serrano, M., and Español, P., 2001, "Thermodynamically Consistent Mesoscopic Fluid Particle Model," Phys. Rev. E, **64**(4), p. 046115.

[12] Sharma, N., and Patankar, N. A., 2004, "Direct Numerical Simulation of the Brownian Motion of Particles by Using Fluctuating Hydrodynamic Equations," J. Comput. Phys., **201**(2), pp. 466–486.

[13] Serrano, M., Gianni, D., Español, P., Flekkøy, E., and Coveney, P., 2002, "Mesoscopic Dynamics of Voronoi Fluid Particles," J. Phys. A, **35**(7), pp. 1605–1625.

[14] Donev, A., Vanden-Eijnden, E., Garcia, A. L., and Bell, J. B., 2010, "On the Accuracy of Explicit Finite-Volume Schemes for Fluctuating Hydrodynamics," Commun. Appl. Math. Comput. Sci., **5**(2), pp. 149–197.

[15] Ladd, A. J. C., 1993, "Short-Time Motion of Colloidal Particles: Numerical Simulation via a Fluctuating Lattice-Boltzmann Equation," Phys. Rev. Lett., **70**(9), pp. 1339–1342.

[16] Ladd, A. J. C., 1994, "Numerical Simulations of Particulate Suspensions via a Discretized Boltzmann Equation. Part 1. Theoretical Foundation," J. Fluid Mech., **271**, pp. 285–309.

[17] Ladd, A. J. C., 1994, "Numerical Simulations of Particulate Suspensions via a Discretized Boltzmann Equation. Part 2. Numerical Results," J. Fluid Mech., **271**, pp. 311–339.

[18] Patankar, N. A., 2002, "Direct Numerical Simulation of Moving Charged, Flexible Bodies With Thermal Fluctuations," Technical Proceedings of the 2002 International Conference on Computational Nanoscience and Nanotechnology, Nano Science and Technology Institute, Vol. 2, pp. 93–96.

[19] Adhikari, R., Stratford, K., Cates, M. E., and Wagner, A. J., 2005, "Fluctuating Lattice–Boltzmann," EPL, **71**(3), pp. 473–479.

[20] Dünweg, B., and Ladd, A. J. C., 2008, "Lattice Boltzmann Simulations of Soft Matter Systems," Adv. Polym. Sci., **221**, pp. 89–166.

[21] Nie, D., and Lin, J., 2009, "A Fluctuating Lattice-Boltzmann Model for Direct Numerical Simulation of Particle Brownian Motion," Particuology, **7**(6), pp. 501–506.

[22] Español, P., and Zúñiga, I., 2009, "On the Definition of Discrete Hydrodynamic Variables," J. Chem. Phys., **131**, p. 164106.

[23] Español, P., Anero, J., and Zúñiga, I., 2009, "Microscopic Derivation of Discrete Hydrodynamics," J. Chem. Phys., **131**, p. 244117.

[24] Atzberger, P. J., Kramer, P. R., and Peskin, C. S., 2007, "A Stochastic Immersed Boundary Method for Fluid-Structure Dynamics at Microscopic Length Scales," J. Comput. Phys., **224**(2), pp. 1255–1292.

[25] Ermak, D. L., and McCammon, J. A., 1978, "Brownian Dynamics With Hydrodynamic Interactions," J. Chem. Phys., **69**(4), pp. 1352–1360.

[26] Brady, J. F., and Bossis, G., 1988, "Stokesian Dynamics," Annu. Rev. Fluid Mech., **20**(1), pp. 111–157.

[27] Foss, D. R., and Brady, J. F., 2000, "Structure, Diffusion and Rheology of Brownian Suspensions by Stokesian Dynamics Simulation," J. Fluid Mech., **407**, pp. 167–200.

[28] Banchio, A. J., and Brady, J. F., 2003, "Accelerated Stokesian Dynamics: Brownian Motion," J. Chem. Phys., **118**(22), pp. 10323–10332.

[29] Iwashita, T., Nakayama, Y., and Yamamoto, R., 2008, "A Numerical Model for Brownian Particles Fluctuating in Incompressible Fluids," J. Phys. Soc. Jpn., **77**(7), p. 074007.

[30] Iwashita, T., and Yamamoto, R., 2009, "Short-Time Motion of Brownian Particles in a Shear Flow," Phys. Rev. E, **79**(3), p. 031401.

[31] Kubo, R., 1966, "The Fluctuation-Dissipation Theorem," Rep. Prog. Phys., **29**(1), pp. 255–284.

[32] Kubo, R., Toda, M., and Hashitsume, N., 1991, *Statistical Physics II: Nonequilibrium Statistical Mechanics*, 2nd ed., Vol. 31, Springer-Verlag, Berlin.

[33] Uma, B., Eckmann, D. M., Ayyaswamy, P. S., and Radhakrishnan, R., 2012, "A Hybrid Formalism Combining Fluctuating Hydrodynamics and Generalized Langevin Dynamics for the Simulation of Nanoparticle Thermal Motion in an Incompressible Fluid Medium," Mol. Phys., **110**(11-12), pp. 1057–1067.

[34] Radhakrishnan, R., Uma, B., Liu, J., Ayyaswamy, P., and Eckmann, D., 2012, "Temporal Multiscale Approach for Nanocarrier Motion With Simultaneous Adhesion and Hydrodynamic Interactions in Targeted Drug Delivery," J. Comput. Phys.: Special Issue on Multiscale Modeling and Simulation of Biological Systems (in press).

[35] Grmela, M., and Öttinger, H., 1997, "Dynamics and Thermodynamics of Complex Fluids. I. Development of a General Formalism," Phys. Rev. E, **56**(6), pp. 6620–6632.

[36] Öttinger, H., and Grmela, M., 1997, "Dynamics and Thermodynamics of Complex Fluids. II. Illustrations of a General Formalism," Phys. Rev. E, **56**(6), pp. 6633–6655.

[37] Patankar, N. A., Singh, P., Joseph, D. D., Glowinski, R., and Pan, T. W., 2000, "A New Formulation of the Distributed Lagrange Multiplier/Fictitious Domain Method for Particulate Flows," Int. J. Multiphase Flow, **26**, pp. 1509–1524.

[38] Chen, Y., Sharma, N., and Patankar, N., 2006, "Fluctuating Immersed Material (FIMAT) Dynamics for the Direct Numerical Simulation of the Brownian Motion of Particles," Proceedings of the IUTAM Symposium on Computational Multiphase Flow, S. Balachandar and A. Prosperetti, eds., Springer-Verlag, pp. 119–129.

[39] Hu, H., 1996, "Direct Simulation of Flows of Solid-Liquid Mixtures," Int. J. Multiphase Flow, **22**(2), pp. 335–352.

[40] Hu, H. H., Patankar, N. A., and Zhu, M. Y., 2001, "Direct Numerical Simulations of Fluid-Solid Systems Using the Arbitrary Langrangian-Eulerian Technique," J. Comput. Phys., **169**(2), pp. 427–462.

[41] Zwanzig, R., and Bixon, M., 1970, "Hydrodynamic Theory of the Velocity Correlation Function," Phys. Rev. A, **2**(5), pp. 2005–2012.

[42] Keizer, J., 1987, *Statistical Thermodynamics of Nonequilibrium Processes*, Springer-Verlag, Berlin.

[43] Zwanzig, R., 2001, *Nonequilibrium Statistical Mechanics*, Oxford University Press, New York.
[44] Heyes, D. M., Nuevo, M. J., Morales, J. J., and Branka, A. C., 1998, "Translational and Rotational Diffusion of Model Nanocolloidal Dispersions Studied by Molecular Dynamics Simulations," J. Phys.: Condens. Matter, **10**(45), pp. 10159–10178.
[45] Happel, J., and Brenner, H., 1983, *Low Reynolds Number Hydrodynamics*, Martinus Nijhoff Publishers, The Hague, The Netherlands.
[46] Mavrovouniotis, G., and Brenner, H., 1988, "Hindered Sedimentation, Diffusion, and Dispersion Coefficients for Brownian Spheres in Circular Cylindrical Pores," J. Colloid Interface Sci., **124**(1), pp. 269–283.
[47] Brenner, H., and Gaydos, L., 1977, "The Constrained Brownian Movement of Spherical Particles in Cylindrical Pores of Comparable Radius: Models of the Diffusive and Convective Transport of Solute Molecules in Membranes and Porous Media," J. Colloid Interface Sci., **58**(2), pp. 312–356.